NanoImpact 19 (2020) 100239

Contents lists available at ScienceDirect

NanoImpact

journal homepage: www.elsevier.com/locate/nanoimpact

Research paper

Unravelling the uptake pathway and accumulation of silver from manufactured silver nanoparticles in the freshwater amphipod *Hyalella azteca* using correlative microscopy

Sebastian Kuehr[a,b], Jessica Klehm[c], Claudia Stehr[c], Matthias Menzel[c], Christian Schlechtriem[a,b,d,*]

[a] Fraunhofer Institute for Molecular Biology and Applied Ecology IME, Schmallenberg, Germany
[b] Department Chemistry and Biology, "Ecotoxicology" Work Group, University of Siegen, Siegen, Germany
[c] Fraunhofer Institute for Microstructure of Materials and Systems IMWS, Halle, Germany
[d] Institute for Environmental Research, RWTH Aachen, Aachen, Germany

ARTICLE INFO

Editor: Chunying Chen

Keywords:
Silver nanoparticles
Bioavailability
Bioaccumulation
Correlative micrsocopy
Hyalella azteca

ABSTRACT

Silver nanoparticles (AgNPs) are known to enter the aquatic environment via leachates from landfills or by the effluent or sludge of sewage treatment plants.

Even if the AgNPs are sulfidized, Ag from these particles was shown to still be available to several species like the benthic freshwater amphipod *Hyalella azteca*. However, it is still unknown if the primary uptake of Ag from these particles occurs mainly by Ag ions, or if the main uptake of Ag is by ingestion of AgNPs and if they can be found in the animal tissues or just in the gut content without any tissue transfer.

To elucidate the main uptake pathway and localization of AgNPs potentially taken up by *H. azteca*, we exposed the amphipods to Ag using AgNP containing sewage sludge or dissolved Ag from $AgNO_3$.

Further, we seperated the exposed animals into two groups. One had direct contact to the AgNPs enriched sludge, allowing them to feed on it, the second group seperated from the sludge by a strainer allowing only indirect contact by potentially released AgNPs or ions.

The animals exposed for 7 days were examined for their total and nano particulate Ag content using (single-particle) inductively coupled plasma mass spectrometry as well as using methods of correlative microscopy. Thus we were able to show, that low amounts of AgNPs were present exclusively in animals with direct contact to the AgNP enriched sludge and only in the region of the gut. No transfer of AgNPs from the gut into the animals tissue was observed by correlative microscopy. However, measurable Ag body burdens in animals from all treatments and groups indicated that ionic uptake is the main uptake pathway for (bio)accumulation of Ag from AgNPs.

1. Background

There is a growing trend for the use of nanoparticles (NPs) in different sectors like electronic industries, medical devices, clothes and more (European Commission, 2013; Future Markets Inc, 2017). The number of products containing NPs increased 25 fold from 2005 to 2010 leading to an increased impact on the environment (Bundschuh et al., 2018; PEN, 2013). A low amount (≤ 2%) of the manufactured NPs entering the environment is released during the production or further processing of the NPs (Gottschalk and Nowack, 2011). The major proportion of the NPs is entering the environment by waste management processes. In the case of silver NPs (AgNPs) 50% of the NPs reach the environment as solid waste like textiles, or packaging waste (Adam and Nowack, 2017). Once deposited at landfills the solid waste releases the AgNPs over time and they can reach the environment via leachates (Bundschuh et al., 2018). The other 50% of AgNPs reaching the environment are released from sewage treatment plants (STP) (Adam and Nowack, 2017), even if the main part is adsorbed by the sewage sludge (Kaegi et al., 2011; Schlich et al., 2013).

As widely described, AgNPs are mainly transformed to silver sulphide (Ag_2S) while passing through the waste water treatment plant (Burkhardt et al., 2010; Impellitteri et al., 2013; Kaegi et al., 2011; Kaegi et al., 2013; Kampe et al., 2018; Kraas et al., 2017; Levard et al., 2012; Lombi et al., 2013). In this form the Ag is hardly soluble and due to the reduced release of Ag^+ and the decreasing trend to generate reactive oxygen radicals at the sulfidized and thus passivated AgNPs

* Corresponding author at: Fraunhofer Institute for Molecular Biology and Applied Ecology IME, Auf dem Aberg 1, 57392 Schmallenberg, Germany.
E-mail address: christian.schlechtriem@ime.fraunhofer.de (C. Schlechtriem).

https://doi.org/10.1016/j.impact.2020.100239
Received 24 February 2020; Received in revised form 4 July 2020; Accepted 6 July 2020
Available online 15 July 2020

surface, the AgNPs are less toxic than pristine AgNPs or dissolved Ag^+ ions (Ag^+) (Bianchini and Wood, 2008; Bianchini et al., 2002; Choi and Hu, 2008; Kim et al., 2009; Liu and Hurt, 2010; Reinsch et al., 2012; West, 1996). Nevertheless, different studies have shown that sulfidized AgNPs or Ag from these transformed particles are still bioavailable for plants (Kraas et al., 2017), nematodes (Starnes et al., 2016), terrestrial isopods (Kampe et al., 2018) as well as for fresh water amphipods like *Hyalella azteca* (Kühr et al., 2018). *H. azteca* is endemic to North and Central America and regularly used for ecotoxicity and bioaccumulation testing, primarily on metals (Alves et al., 2009a; Kühr et al., 2018; Nuutinen et al., 2003; Othman and Pascoe, 2001; Raths et al., 2020; Schlechtriem et al., 2019). Due to the fact, that sewage treatment plants (STPs) are the main pathway for NPs to enter the aquatic environment, chronic exposure studies with *H. azteca* were carried out on the accumulation of silver from AgNPs in sewage treatment plant effluents (Kühr et al., 2018). It was shown that accumulation of silver in the body of test animals is clearly dependent on the pretreatment of the AgNPs. Accumulation of silver ions (Ag^+) released from AgNPs is assumed to be the major pathway leading to the observed body burden (Kühr et al., 2018). However, it can only be speculated whether ingested AgNPs are also bioavailable and how and to what extent they contribute to the body burden, in contrast to Ag^+.

In this study, exposure tests with *Hyalella azteca* were carried out to elucidate the main uptake pathway, as well as the form and localization of Ag present in the animals. The exposure system used in a previous study (Kühr et al., 2018) was adjusted to allow investigations on the uptake of Ag by *H. azteca* either by direct or indirect contact to sewage sludge from a model STP containing Ag/AgNPs. In addition a comparison between animals exposed to $AgNO_3$ at comparable aqueous Ag concentrations as found in the studies with AgNPs was carried out. The exposed animals were examined for their total Ag body burden and accumulation factors were calculated taking account of the Ag concentrations in the water. Further animals were examined for the presence of AgNPs in the animal tissue. Mild methods were used for i) extraction of AgNPs from the animal tissue to allow investigations by single particle inductively coupled plasma mass spectroscopy (spICP-MS) and for ii) embedding of the animals for examinations by correlative microscopy.

2. Materials and methods

2.1. Handling of AgNP and preparation of the NP stock suspension

NM 300 K, a representative test and reference material from the European Commission's Joint Research Centre and in the scope of the OECD Working party on Manufactured Nanomaterials Sponsorship Program was used for the studies. The material was provided by the Fraunhofer Institute for Molecular Biology and Applied Ecology IME. Summarized information on the characterization and physico-chemical properties can be found in the JRC Report (Klein et al., 2011). The production of the AgNP working suspension to be applied to the model STP and to spike control sludge was carried out as described by (Kühr et al., 2018). The stock suspension was diluted with ultra high quality water (UHQ water), hand-shaken for 1 min and sonicated for 15 min (640 W) (Bandelin, Sonorex) to disperse the AgNPs and to carefully homogenize the suspension. $AgNO_3$ (purity of > 99.9%) was purchased as a salt from Carl Roth and dissolved and diluted using ultra-high quality water (UHQ water) to prepare the $AgNO_3$ stock solution.

2.2. Sewage sludge exposure and preparation of feeding filters

For our study we used the same sewage sludge as used by Kampe et al. (2018) from a lab scale STP simulation according to OECD TG 303A (Organisation for Economic Co-operation and Develpement (OECD), 2001). The sludge was examined by transmission electron microscopy (TEM) using energy dispersive x-ray spectroscopy (EDX). It was shown, that the AgNPs were metallic, still of comparable size as the pristine AgNPs from the NM 300 K stock suspension, but completely transformed into Ag_2S according to Kampe et al. (2018).

One batch of sludge from an STP run treated with AgNP (S_L), and pure sludge from a control STP run (S_0) were suspended in UHQ water for the preparation of food filters for the exposure tests (for further information see SI SA.). All sludge suspensions were homogenized using a disperser (IKA® T25 digital ULTRATURRAX®) and stirred for 3 h before being filtered through glass microfiber filters (Whatman® GF 6, 50 mm) by using a vacuum pump (Vacobox, KNF) as described by (Kühr et al., 2018) to achieve a loading of 50 to 80 mg (dry mass). The loaded filters were frozen and stored at −20 °C before being used.

2.3. Hyalella azteca

The freshwater water amphipod *H. azteca* was taken from the stock culture of Fraunhofer IME, Schmallenberg. The strain was originally obtained from "Freds Haustierzoo "(Cologne, Germany). The culturing procedure was carried out according to (Kühr et al., 2018) using reconstituted water containing bromide (Alves et al., 2009b). The stock culture was kept in 2 L flasks filled with reconstituted water containing bromide (Alves et al., 2009b), each containing 30 adult animals. Three times a week, 5 mg of ground fish feed (Tetramin®, Tetra) were added to each beaker to maintain optimal growth of the test animals. A small piece of gauze (3 × 3 cm) was added to provide a place of refuge. Juveniles were separated from the parent animals once a week to be cultured separately until used in tests. Only healthy amphipods free from observable diseases and abnormalities were used in these studies.

2.4. First exposure study (7d)

The first exposure study with NM 300 K was carried out with adult animals (at least 8 weeks old). In this test one Ag-treatment and a control treatment were compared (Table 1). Every treatment consisted of 5 test groups with 20 adult *H. azteca* each kept in 600 mL glass beakers filled with 500 mL copper reduced tap water (Fig. 1). In each beaker an additional group of 5 adult animals was separated from the major group by a stainless steel strainer. The group within the strainer was fed control sludge (S_0), while the major group outside the strainer was fed with sludge treated with AgNP (S_L). Animals were exposed for 7 days without water exchange. The sludge coated filters were added to the beakers 24 h before the animals were added to allow Ag^+ ions to be released into the media, even if the time was too short to enable the system to equilibrate. Water samples (n = 3, each 10 mL) for Ag measurement were taken at the start (before animals were added), at day 4 and at the end of the test (day 7) from the beaker near the strainer. The water samples were analysed directly after ultracentrifugation (for further information see SI SB). The filtrate was used

Table 1
Ag content in sludge [mg Ag/kg] and TWA concentrations of the test media [µg Ag/L]. Sludge samples were measured once (n = 5) for all treatments/tests. * sludge in strainer was S_0 sludge, ** $AgNO_3$ solution;

Study	Treatment	Matrix	TWA in medium [µg Ag/L]	Concentration in sludge [mg Ag/kg]
Exposure study I	S_0	Media	–	
		Sludge		1.17 ± 0.05
	S_L	Media	5.11	
		Sludge		7303 ± 873*
Exposure study II	S_0	Media	–	
		Sludge		1.17 ± 0.05
	S_L	Media	16.74	
		Sludge		7303 ± 873*
	$AgNO_3$	Media	5.41**	
		Sludge		1.17 ± 0.05

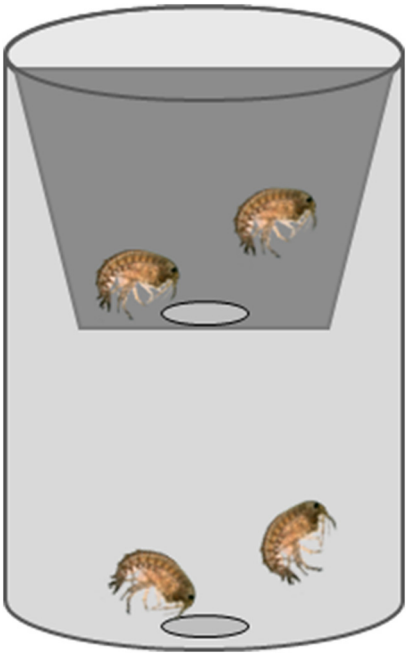

Fig. 1. Schematic overview of the exposure scenario including two groups of *H. azteca*, separated by a strainer to provide direct (bottom) or only indirect (top) contact to AgNPs present in sewage sludge loaded on glass fiber filter. The group within the strainer was fed control sludge.

to measure the concentration of Ag^+, while the filter residue was analysed for its Ag content as an indication of AgNPs in the water phase. The animals were collected at the end of the exposure phase, frozen with liquid nitrogen and stored at −80 °C until histological preparation for correlative microscopy and measurements using inductively coupled plasma mass spectrometry (ICP-MS) as described below. The measurement of the total Ag content of the water samples was carried out before and after ultrafiltration. Only the water samples for the measurement of total Ag content were acidified by adding 200 µL of nitric acid (69%, suprapure grade, Roth).

2.5. Second exposure study (7d)

A second exposure test was carried out under similar conditions as described before but including an additional treatment using control sludge only. In this treatment $AgNO_3$ solution was applied as the aqueous test medium mirroring the time weighted average concentration of Ag in the water measured during the first exposure test with sludge containing AgNPs (S_L) (nominal Ag concentration: 5.11 µg/L). Animals and water samples collected during the study were handled as described before. Further replicate beakers (n = 3) were used for examination using single-particle ICP-MS (spICP-MS). Animals were frozen using liquid nitrogen and stored at −80 °C. Water samples (10 mL, n = 3 for each treatment and sampling point) for total Ag measurement were taken at the start (before animals were added), at day 4 and at the end of the test (day 7) from inside the strainer and from outside near the bottom of the beaker. The water samples were prepared and measured as described above directly and after ultrafiltration. Water samples for analysis using spICP-MS (n = 3 for each treatment and sampling point) were taken at the test start from the fresh media and at the end of the test from the aged media, and were measured directly after sampling.

2.6. Determination of total silver concentrations in the aqueous test media, sewage sludge and Hyalella azteca samples

Collected samples of aqueous test media were prepared and analysed as described by Kühr et al. (2018), for further information see SI SB. To meausure the total Ag content of sewage sludge loaded on glass fiber filters, disposable scalpels (Braun, Cutfix®) were used to remove sludge samples from the filter surface (n = 5 for each treatment; one single filter = one replicate). The analysis of total Ag concentrations in sewage sludge and *Hyalella azteca* (n = 5 for each treatment; each replicate contained 15 to 18 pooled animals) collected during the studies were carried out according to Kühr et al. (2018) and (Wasmuth et al., 2016) (for further information see SI SC). The analysis of total Ag concentrations in the sludge was only carried out before exposure.

2.7. Examination of Hyalella tissue and aqueous test media by single particle ICP-MS

For the examination of *Hyalella* tissue by single particle ICP-MS (sp-ICP-MS) a gentle sample preparation method was applied that does not dissolve the particles and that affects the particle properties as little as possible. For this, tissue samples (n = 3 for each treatment) were digested using the enzyme proteinase K according to the method described by (Loeschner et al., 2013) and (Schmidt et al., 2011). The dried animals (10 pooled animals per replicate) were transferred to a 50 mL glass beaker and gently pressed using a glass rod to destroy the carapax and allowing the enzyme to enter the body and digest the proteins. The glass rod was rinsed with 10 mL of the digestion solution (45 mg proteinase K in 1 L buffer solution + 0.5% SDS + 50 mM NH_4HCO_3, pH adjusted to 8.0–8.2) which was obtained from the glass beaker containing the crushed tissue samples to minimize the potential loss of any silver via glass rod. The samples were incubated in the 10 mL digestion solution for 3 h at 50 °C and 100 rpm. This process has no or only a negligible impact on the dissolution and size distribution of the NM 300 K NPs (Kuehr et al., 2020). The incubated digestion solution was filtered using 0.45 µm syringe filters (Minisart® NML, 0.45 µm) before analysis. The sp-ICP-MS analysis using an ICP-QQQ-MS (Agilent 8900, Agilent Technologies, Waldbronn, Germany) were carried out as described by (Kuehr et al., 2020) (for further information see SI SD). Due to poor analytical quality controls and incomplete digestion of the animal tissues, the quantitative values of the particle numbers can only be seen as a rough assessment, to elucidate the differences in particle concentrations in the different treatments (e.g $AgNO_3$ vs S_L-media or tissue). After measurement of particle concentrations in the digested fraction using sp-ICP-MS, the filtered solution was further digested by aqua regia to allow analysis of total Ag content. For digestion, 2 mL of aqua regia were added to 5 mL of the filtered solution prior to digestion in a microwave as described above (turboWave® Inert, MLS; max temperature 220 °C, max pressure 40 bar). Only half of the collected animals were processed and analysed as described above. The non-enzymatically digested part of the samples (n = 3, each consisting of 10 pooled animals) was also digested using aqua regia (8 mL) using the same microwave method. Both solutions obtained were measured for their total Ag content. This allowed comparison of the content of Ag in the protein fraction of the animals with the whole amount of Ag from the complete samples (including AgNPs attached to the carapace etc.). Aqueous media samples collected during the studies were measured following the same procedure but without enzymatic digestion.

2.8. Imaging of AgNPs in Hyalella azteca by correlative microscopy

Correlative microscopy, combining the power and advantages of different imaging systems, e.g., light microscopy, electron microscopy, X-ray, etc., has become an important tool for material and life science during the last years. Using correlative microscopy additional information can be obtained at the same sample site because different complementary information can be spatially assigned and different orders of magnitude related to resolution and image field can be recorded (Caplan et al., 2011; Loussert Fonta and Humbel, 2015). Electron microscopy provides high resolution but has one central limitation

with a restricted field of view. Light microscopy has the advantage of having a large field of view which enables identification and localization of structures at low magnification (Loussert Fonta and Humbel, 2015). The combination of these two imaging techniques is a valuable approach to investigate structures at a submicrometer level in biological research (Bradley and Withers, 2016; Guérin et al., 2019; Verkade and Collinson, 2019).

In this study, correlative microscopy was used for morphological imaging of silver nanoparticles in *H. azteca*. After appropriate sample preparation, investigations at the macrometer to nanometer level were carried out by combining microscopic techniques and X-Ray diffraction analysis (micro computer tomography). This allowed evaluation of the state of tissue structures following preparation by different techniques as well as imaging the morphology of the nanoparticles and to detect their localization. Additionally, EDX was applied for the elemental analysis or chemical characterization of the samples. For a schematic overview of correlative micrcoscopy see SI Fig. S1.

In order to get an impression of the morphology of the nanoparticles used in this study, SEM investigations were carried out on the raw material (Fig. S2). For this purpose the Ag nanoparticles were diluted (100 µg/L), dispersed using ultrasound and applied to a glass slide for SEM investigations. The diameter of the Ag nanoparticles was determined to be between 18 and 20 nm.

An adapted sample preparation protocol was developed to enable investigations by correlative microscopy (Mulisch and Sauer, 2015). The experimental animals were embedded in polymethylmethacrylate (PMMA). During the embedding process, a staining technique was applied. Two staining protocols based on either osmium tetroxide or iodine were tested.

The embedded samples ($n = 10$ for each treatment, single animals) were subsequently examined by using micro computed tomography (equipment nanome|x 180NF) to assess the embedding quality and the determined macro- and microstructure. It was found that staining with osmium tetroxide can cause localized damage such as structural changes at the micrometer level (Fig. 2, left). However, the iodine stained samples showed no damage and iodine staining was thus the preferred procedure used in this study (Fig. 2, right).

For imaging by light and electron microscopy, a further sample preparation was carried out. Thin sections of the embedded samples with a thickness of about 80 µm were prepared according to the cutting-grinding technique of Karl Donath (Donath, 1995). The sections were analysed by light (Olympus BX 51) and scanning electron microscopy (SEM, equipment Quanta 3D FEG, FEI) to identify areas in the morphological structure of the animals where the nanoparticles could be located. Such areas were subsequently analysed by SEM combined with EDX to detect and localize silver. Images were produced using backscattered electron (BSE) material contrast in the low vacuum mode at an accelerating voltage of 10 kV after conductive coating with carbon. An additional sample preparation was conducted to allow further investigations by transmission electron microscopy (TEM, equipment FEI Tecnai G2 F20). The identified areas were dissected with an ultramicrotome [equipment RMC PowerTome PT-PC with CRX cryochamber (RMC, Tucson)] with a diamond knife (DIATOME angle 35°) to generate ultra-thin sections of 50 nm. Subsequently, TEM investigations were performed in combination with EDX analysis for the detection of silver nanoparticles (EDX Nanospot). For each sample at least 3 images were examined and each region of interest (see below) was examined at least 3 times.

2.9. Data analysis

The data analysis software Origin (OriginLab Corporation; OriginPro 2017G) was used for analysis of variance (ANOVA) for the data obtained in the different studies. All data were subjected to an outlier test (SQS 2013 Version 1.00 by J. Kleiner and G. Wachter). Replicates identified as an outlier were excluded from further data analysis. Time weighted average concentrations (TWA) of Ag in the aqueous phase of the different treatments were calculated for the experimental periods. Accumulation factors (AF_M) were obtained by dividing the total Ag concentrations in the amphipods by the TWA concentrations of the test medium AF_M. Due to the lack of evidence for obtaining steady-state conditions during the exposure studies, the calculated AF_M values do not necessarily reflect equilibrium conditions.

3. Results

3.1. First exposure tests

In the first exposure test (7d) with S_L sludge (7303 ± 873 mg Ag/kg) a TWA concentration of 5.11 µg Ag/L was measured in the water (Table 1, Table S1). In comparison, no measurable Ag concentration was present in the media of the S_0 treatment.

Animals collected at the end of the first exposure test (7d) from the S_0 treatment showed a negligible total Ag content (Fig. 8) independent of whether they were kept in the strainer (0.03 ± 0.03 mg Ag/kg) or at the bottom of the beaker (0.04 ± 0.03 mg Ag/kg). The animals which were kept in the strainer of the S_L treatment, without direct contact to the Ag/AgNP containing sludge, showed a low Ag body burden of 1.92 ± 0.82 mg Ag/kg. However, for the animals with direct contact to the S_L sludge, a high body burden of 201.36 ± 33.25 mg Ag/kg was measured (Fig. 8).

Accumulation factors were calculated as the ratio of tissue concentrations to medium (AF_M) concentrations for the first exposure test (Table 2). Due to non-measurable Ag concentrations in the media of the control group no AF_M could be calculated. In contrast, AF_M values of 376 and 39,404 were calculated for the strainer group fed control sludge and the bottom group of the S_L treatment, respectively (Table 2).

3.1.1. Histological investigations using correlative microscopy

Two staining protocols based on osmium teroxide or iodine were

Fig. 2. Comparison of OsO_4 (left) and iodine (right) staining techniques via CT investigations.

Table 2
Calculated AF_M values for the amphipod groups in the two exposure studies.

Study	Treatment	Group	AF_M
Exposure Study I	S_0	Strainer	–
		Bottom	–
	S_L	Strainer	376
		Bottom	39,404
Exposure study II	S_0	Strainer	–
		Bottom	–
	S_L	Strainer	504
		Bottom	21,730
	$AgNO_3$	Strainer	363
		Bottom	396

tested to prepare the embedded experimental animals for correlative microscopy. Investigating the stained samples by CT showed that the iodine staining is obviously better suited for the maintenance of the tissue as described above (Fig. 2). Due to the size of the applied AgNPs the imaging of the Ag nanoparticles in the iodine stained *H. azteca* by CT would only have been possible after agglomerate formation. However, this could not be confirmed by the CT images which indicated a good dispersion of potentially ingested AgNPs even after direct exposure to NP enriched sewage sludge (Fig. 3, video material Video S1 and Video S2).

Using correlative microscopy, the morphology of *H. azteca* from the macro- to nanometer level of the thin and ultra-thin sections was investigated. Inspection of the SEM images showed that the nanoparticles were present in the intestine of the animals with direct contact to AgNP enriched sludge (S_L). Thus, this region (intestine and gut content) (ROI: region of interest) was noted for further investigations (Fig. 4; A).

The analysis with EDX in SEM showed a peak of Ag in the ROI (Fig. 4; C). This was confirmed by TEM investigations at a higher resolution after cutting the same region with an ultramicrotome. This nanospot analysis indicated an enormous Ag deflection during EDX analysis at the nanometer level, which confirmed the results obtained at the micrometer level in the SEM (Fig. 5).

SEM images of *H. azteca* (S_L treatment) with indirect contact to Ag during the first exposure test showed particles which are similar to the raw material of the applied nanoparticles in the intestine of the animals. However, this was not confirmed by the EDX analyses where no silver was detected but traces of P and Ca were found (Fig. 6). This was confirmed by the nanospot analyzes in the TEM (Fig. 7). Only a clear peak of Cu, potentially originating from the Cu-grid used in the ultramicrotome work, was observed.

3.2. Second exposure test

Considering the TWA Ag concentration measured in the media of the S_L treatment during the first exposure test (5.11 µg Ag/L; Table S1) a similar Ag media concentration was established for the $AgNO_3$ treatment with 5.41 µg Ag/L (Table S2). However, the TWA Ag

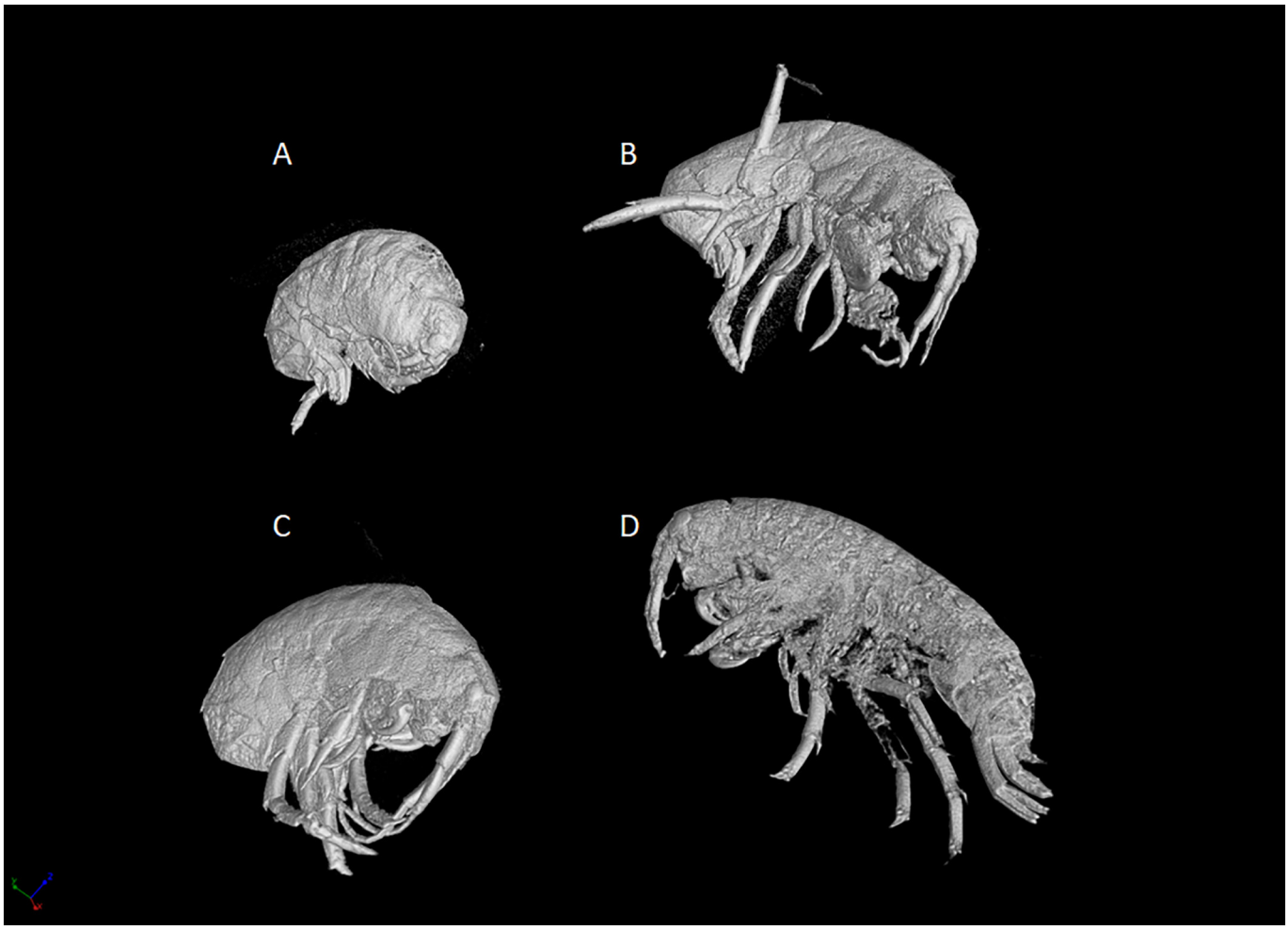

Fig. 3. 3D imaging after CT investigations of iodine stained *H. azteca*. Agglomerates or aggregates of NPs > 400 µm would have been visible as coloured dots. A: Hyalella from the strainer of S_L treatment; B: Hyalella from the bottom of the S_0 treatment; C: Hyalella from the bottom of the S_L treatment; D: Hyalella from the strainer of the S_0 treatment. Comparable to Video S1.

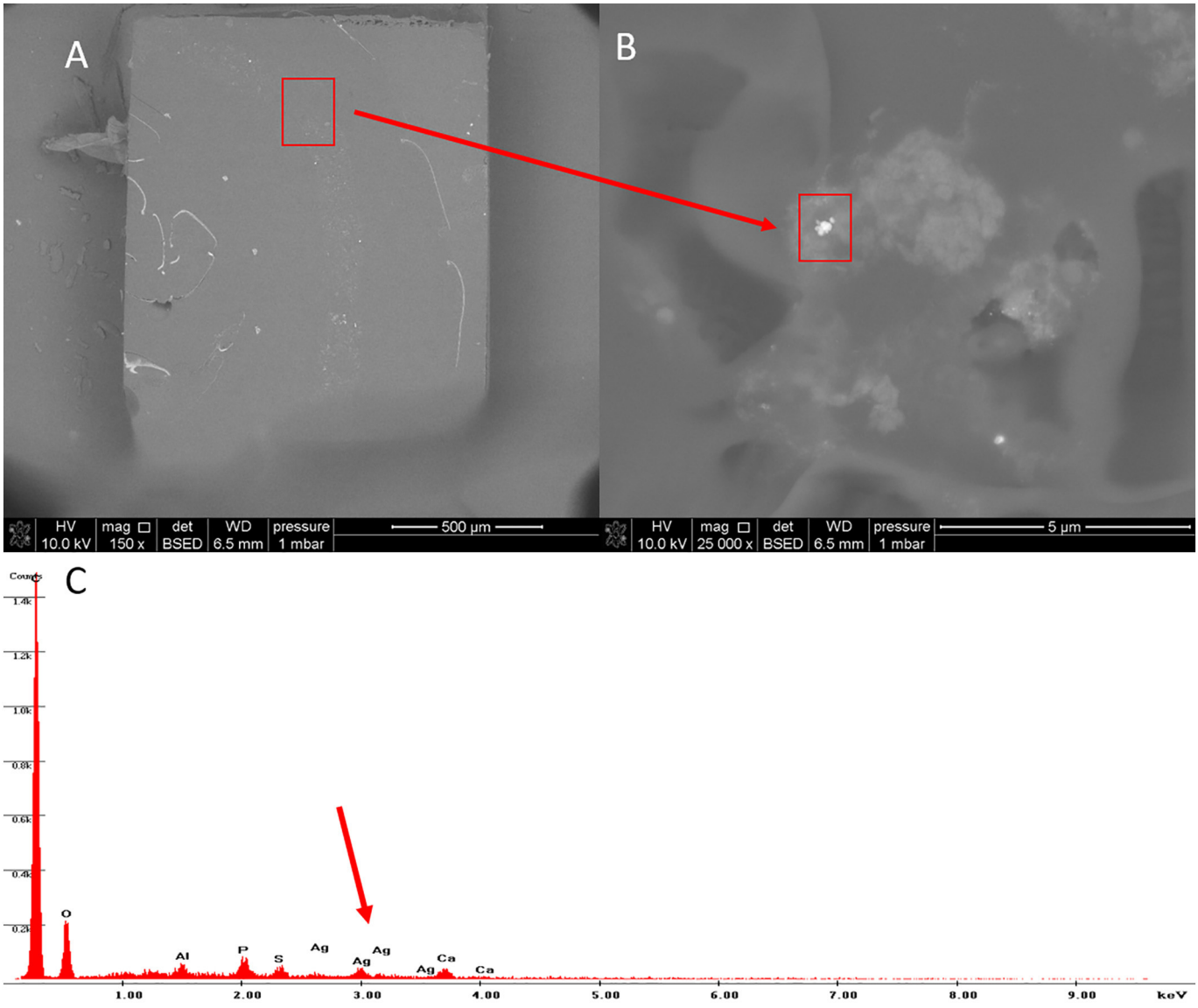

Fig. 4. SEM image of the intestine region of *H. azteca* from S_L treatment (first exposure test) with direct contact to the AgNPs enriched sludge. Marked ROI (red square) at A: gut content 150 x magnification and B: 25000 x magnification of the region from the red square of part A and EDX spectrum (C) with Ag peak (red arrow, bottom). (For interpretation of the references to colour in this figure legend, the reader is referred to the web version of this article.)

concentration of the S_L treatment measured in the medium during the second exposure test was 16.74 µg Ag/L (Table S3) and thus around three times higher as compared to the first exposure test. Only the samples from day 7 of the S_L treatment showed a significant difference in media concentrations between bottom and strainer region (Table S4). There were no significant differences in $AgNO_3$ media concentrations measured at the bottom or in the strainer (Table S5). In both treatments, most of the particulate Ag or Ag^+ in the medium (around 99%) were supposed to be bound to organic colloids or precipitated as shown by the media concentrations measured after ultracentrifugation (Table S2 and S3). In agreement with the first exposure test, no measurable Ag concentration was present in the media of the S_0 control sludge treatment (Fig. 8).

The control animals of the second exposure test (7d) showed very low Ag tissue concentrations of 0.03 ± 0.02 mg Ag/kg and 0.18 ± 0.00 mg Ag/kg for the animals in the strainer and at the bottom of the beaker, respectively (Fig. 8). For the animals in the $AgNO_3$ treatment low Ag tissue concentrations were determined with 2.14 ± 0.27 mg Ag/kg and 1.96 ± 0.46 mg Ag/kg for the animals at the bottom of the beaker and in the strainer, respectively. The Ag concentrations in the animal tissue from the S_L treatment were higher than those from the first exposure study with 357.91 ± 77.09 mg Ag/kg and 8.31 ± 2.72 mg Ag/kg measured in animals with direct and indirect (strainer group) contact to the S_L-sludge, respectively (Fig. 8).

Also during the second exposure test no AF_M could be calculated for the control animals (fed with S_0 sludge only) due to the non-measurable Ag concentrations in the test media.

AF_M values of 504 and 21,730 were calculated for the animals collected from the S_L treatment (strainer and bottom, respectively). Lower AF_M values were determined for the two groups in the $AgNO_3$ treatment, with similar values of 363 and 396 for the strainer and bottom groups, respectively.

3.2.1. Measurement of total Ag in protein extracts of Hyalella after enzymatic protein digestion

At the end of the second exposure test, a small group of animals was

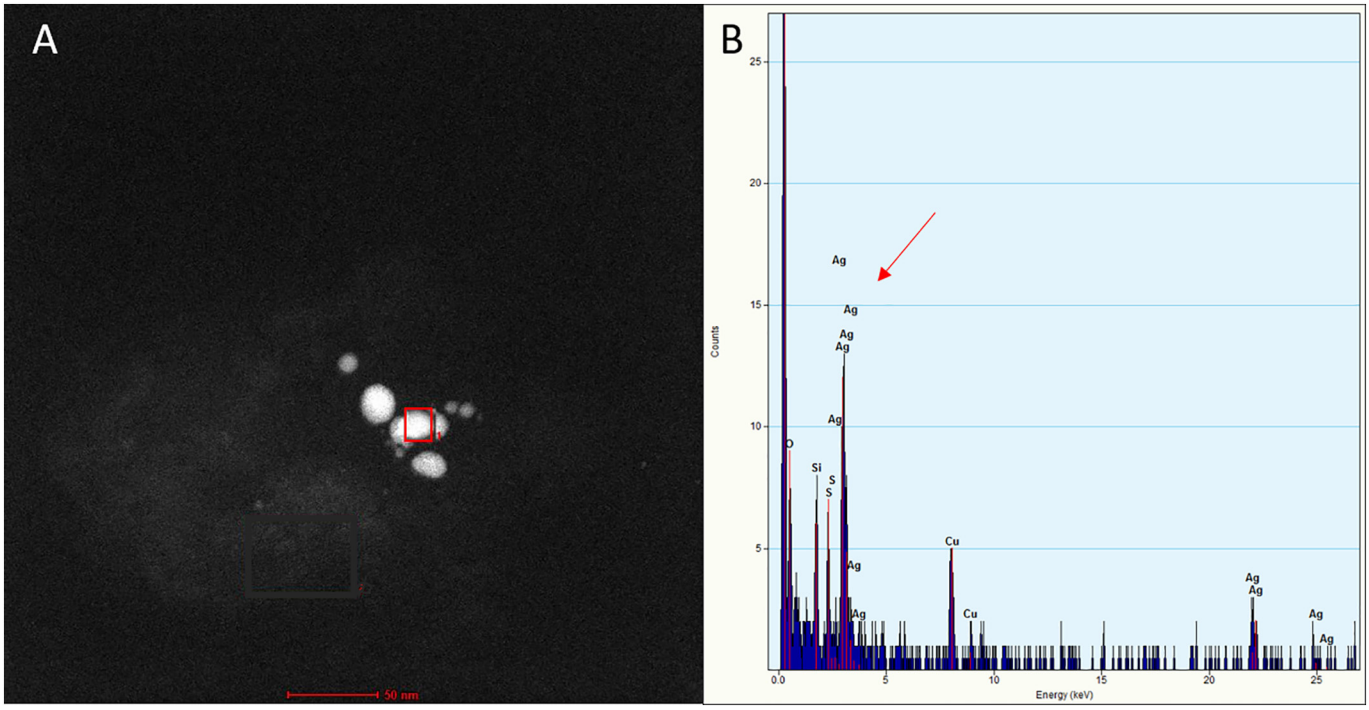

Fig. 5. A: TEM image of ROI after cutting with ultramicrotom and B: EDX spectrum of nanospot analysis with high Ag deflacltion.

collected from each treatment (same replicate beakers) to be enzymatically digested as described for the sp-ICP-MS samples. The total amount of Ag that was extracted with the proteins from the amphipods body was acid digested and determined using ICP-OES. For the $AgNO_3$ treatment, 57% of the total amount of Ag measured in the whole amphipods turned out to be extractable from the protein fraction. The total amount of silver (100%) was equivalent to the concentration measured after acid digestion of the whole animals. However, from the animals of the S_L treatment only 17% of the total amount of silver measured in the whole animals was extractable after enzymatic protein digestion.

3.2.2. Examination of aqueous test media and Hyalella tissue using single particle ICP-MS

By using sp-ICP-MS the number and mean size of Ag particles in the medium and animal samples collected during the second study were determined. Particle concentrations were determined in the media of S_L and $AgNO_3$ treatment. In both treatments the particle concentration increased during the exposure period. In the animal tissue from all treatments including the S_0 sludge particle concentrations were determined at the end of the test (day 7) with the highest value in the S_L treatment. The calculated mean particle sizes were determined for medium and tissue samples and are presented in Table 3.

4. Discussion

AgNPs reach the aquatic environment mostly as transformed hardly soluble silver sulphide (Ag_2S) after passing through the STP. It was recently reported that Ag from AgNPs, which are transformed and believed to be passivated, is still available for uptake by invertebrates exposed to STP effluents or sludge (Kampe et al., 2018; Kühr et al., 2018). This was confirmed in this study which was aimed at elucidating the pathways leading to the accumulation of silver from STP sludge containing AgNPs in *H. azteca*. The dietary uptake of AgNPs from the sludge as well as bioconcentration following dissolution of Ag^+ ions from the AgNPs was observed. However, no tissue penetration and accumulation of ingested particles was shown. This is in accordance with Zeumer et al. (2020) where the dietary uptake of wastewater borne AgNPs obviously did not lead to significant accumulation of Ag.

The AgNP containing sewage sludge used was obtained from a lab scale STP simulation unit running with NM 300 K spiked artificial influent according to OECD TG 303A (Organisation for Economic Co-operation and Develpement (OECD), 2001). The sludge was examined by TEM and EDX revealing that the AgNPs which were still present were sulfidized according to the authors (Kampe et al., 2018). The sludge used for the control groups (S_0) was taken from a control lab scale STP unit running on unspiked artificial influent. The measured total Ag content of around 1.2 mg/kg in the S_0 sludge should result from the initial active sludge used to inoculate the STP units obtained from a municipal STP (Kampe et al., 2018).

In all tests with STP sludge containing AgNPs measurable total Ag concentrations in the test media were found. With the $AgNO_3$ treatment an exposure scenario could be established which was comparable to the media concentrations measured in the STP-sludge treatment (S_L) of the first exposure test. The examination of the test media collected at the start of the second exposure tests using spICP-MS revealed that Ag particles were detected in the S_L and in the $AgNO_3$ treatments. The calculated median size of the particles detected in both media (aqueous phase) was nearly the same. However, a lower particle concentration was determined for the S_L treatment including STP sludge containing AgNPs. Kuehr et al. 2020 also observed Ag particles in an $AgNO_3$ exposure medium with comparable particle sizes. The observation was explained by the measurement of pseudo (presumable) particles (Kuehr et al., 2020) which is the result of two limitations of the spICP-MS method. First, the method cannot distinguish between the manufactured AgNPs and products of Ag^+ precipitations processes like e.g. AgCl or Ag_2S, or higher numbers of Ag^+ attached to colloids or proteins. Second, due to the small size of the NM 300 K AgNP that is near the instrumental size detection limit (around 10 nm for Ag, given by the Agilent MassHunter Software) or the particle detection limit of 16–20 nm as reported by (Lee et al., 2014). Also, the particles detected in the media collected at the start of the second exposure test were supposed to be pseudo particles. In the $AgNO_3$ treatment, which was carried out with control sludge containing no AgNPs, the detected particles could be Ag^+ that was complexed or associated with organic

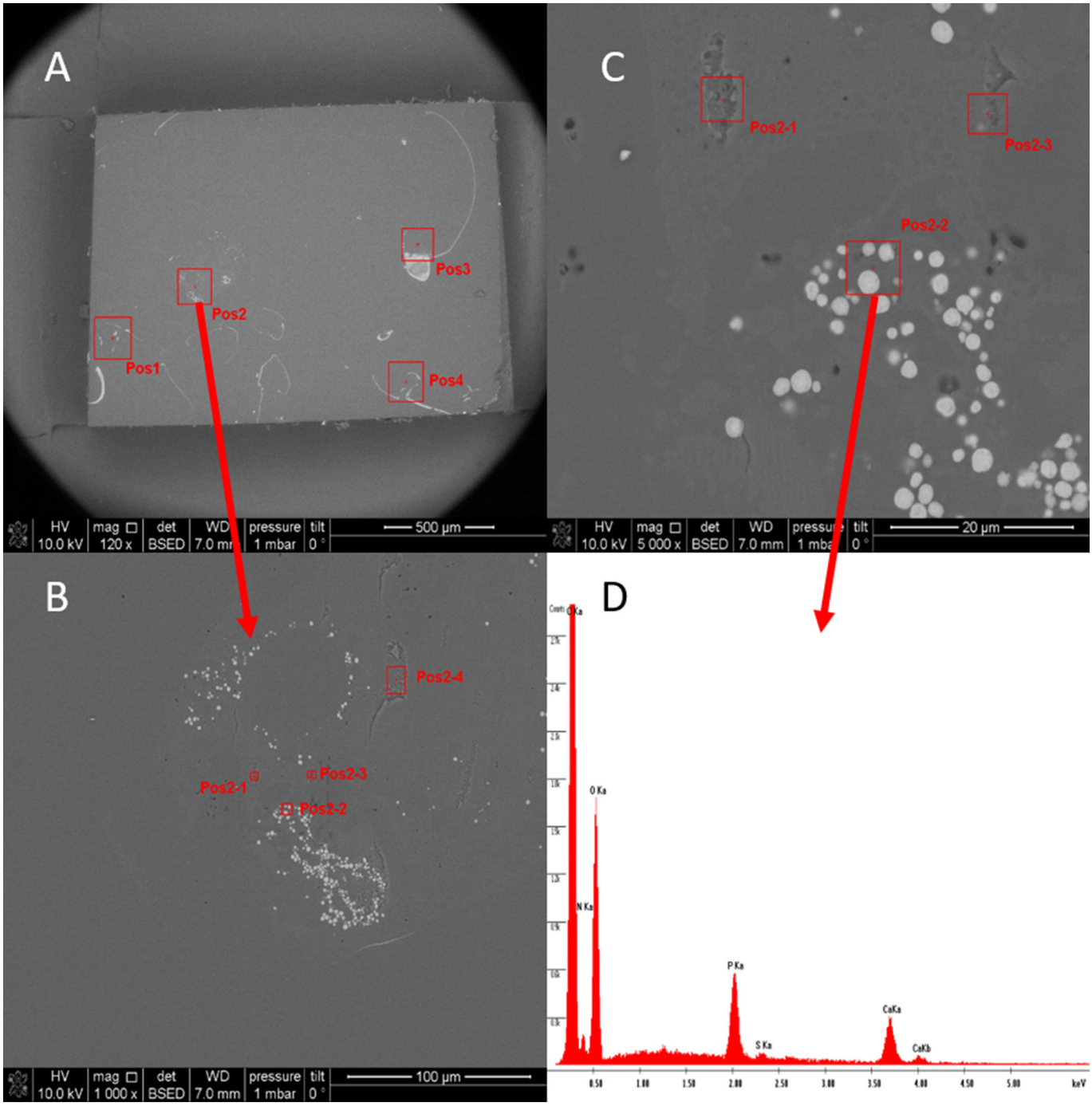

Fig. 6. SEM image of embedded *H. azteca* from S_L treatment (first exposure test) without direct contact to the AgNPs enriched sludge (strainer group) with marked ROIs (red squares, intestine and near region) at 120× (A), 1000× (B) and 5000× magnification (C) with EDX spectrum showing peaks for P and Ca but not for Ag (D). (For interpretation of the references to colour in this figure legend, the reader is referred to the web version of this article.)

or inorganic colloids or precipitated Ag species like Ag_2S or AgCl (Degenkolb et al., 2018). Sulfidized AgNPs are still capable of releasing Ag^+ as described by Kampe et al. (2018) and Kühr et al. (2018). Particles detected in the S_L medium at the test start could be explained by the release of AgNPs from the STP sludge or by Ag^+ ions leaching from the AgNPs and following the same complexation pathway as described before. In the aged medium collected at the end of the second exposure test, nearly the same concentration of Ag particles was measured for the $AgNO_3$ medium. These pseudo particles showed a slightly higher calculated diameter, probably caused by a higher amount of Ag^+ associated with the colloids present compared to those measured at the test start. In contrast, the measured particle concentration in the aqueous media of the S_L treatment was three magnitudes higher in the aged media collected at the test end compared to the concentration in the fresh medium (after 24 h of aging) from the test start. Also the median particle size was higher compared to the test start and in comparison to the particles detected in the $AgNO_3$ medium, but nearly identical to the size of pristine particles (NM 300 K) and to the sulfidized particles measured in the S_L sludge by Kampe et al. (2018). Thus the particles which were measured at the test start were assumed to be an artifact similar to the particles found in the $AgNO_3$ medium.

Measurement of total silver concentrations in exposed animals

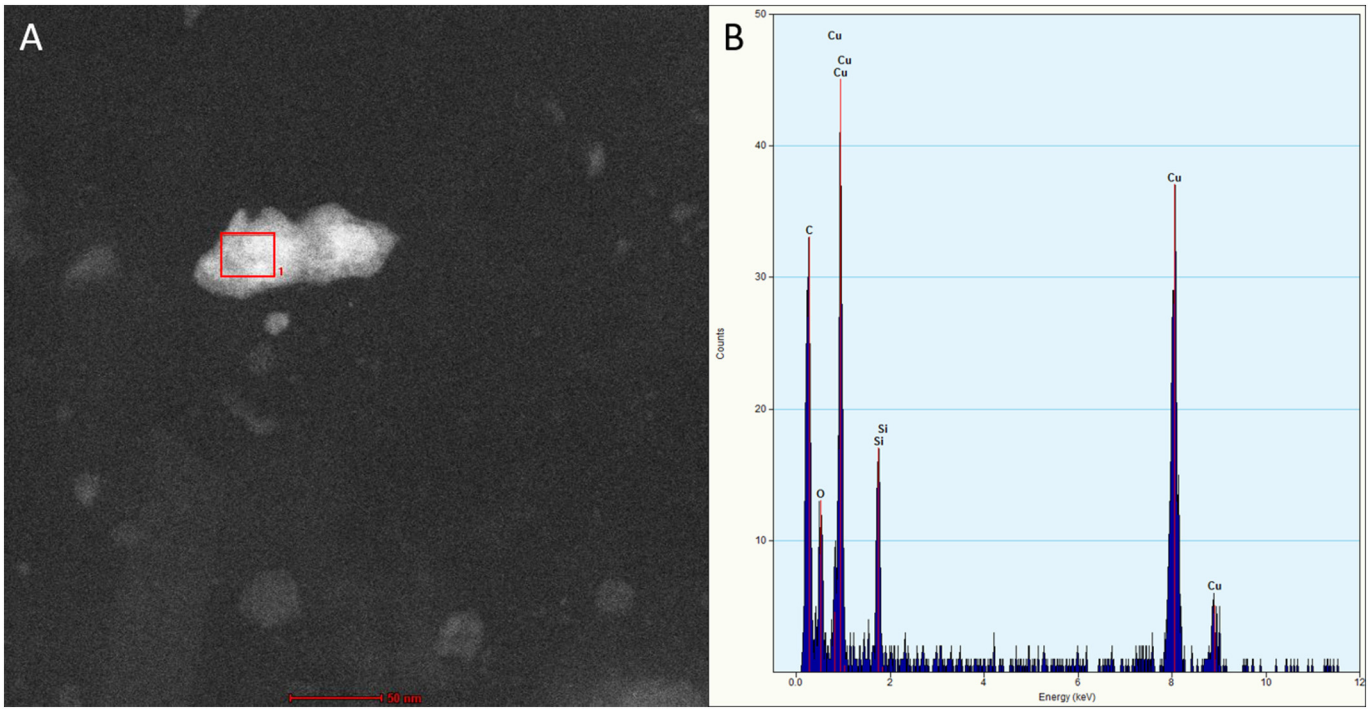

Fig. 7. TEM image of conspicuous (Figure 6) of an animal from the S_L treatment (first exposure test) without direct contact to the AgNPs enriched sludge (strainer group) showing high Cu but no Ag peak in the EDX spectrum (B).

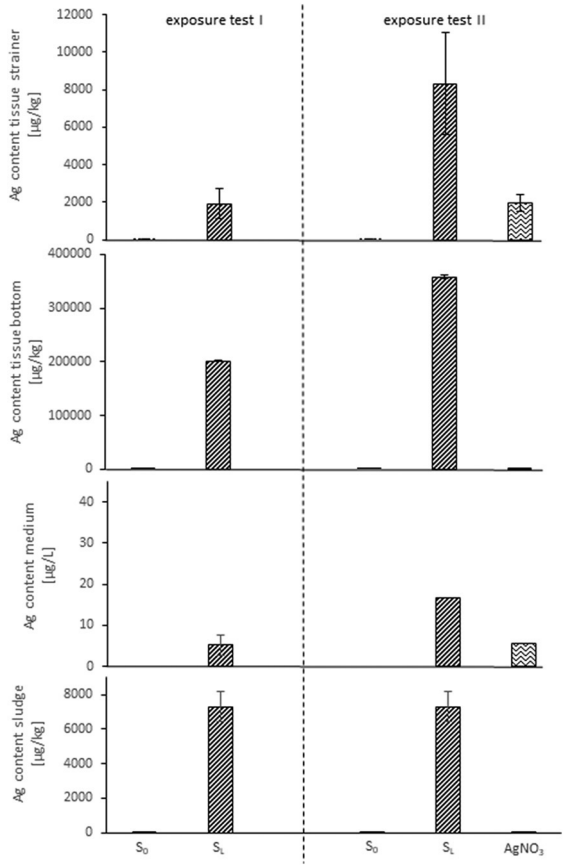

Fig. 8. Exposure test I-II. Measured total Ag concentration in sludge [mg/kg], media [µg/L] and tissues of experimental animals collected from groups exposed outside (bottoms) or inside the strainer (top) (Fig. 1).

showed that the highest tissue concentrations were observed in animals which were in direct contact with the contaminated sludge. Animals obviously ingested AgNPs as part of their diet. This was confirmed by single particle ICP-MS which was carried out to elucidate the presence of ingested particles in the previously exposed animals. Highest particle concentrations were measured in the animals which had access to contaminated sludge. However, particles could also be detected in animals of the $AgNO_3$ treatment and even in control animals. The spICP-MS method applied in this study is only suitable to prove the presence of AgNPs with a particle size > 20 nm. In addition, a differentiation between real AgNPs and measuring artifacts by the spICP-MS caused by high amounts of ions in the sample background is not possible. Thus, it cannot be excluded that the measured particles were only the result of an artifact due to the limitations of the measurement and calculation process of the spICP-MS. Due to the sample fitration using 0.45 µm syringe filters, we cannot exclude that particles or agglomerations of particles with a size higher than 450 nm had not been available for the spICP-MS measurements. However, such big particles would have been visible at least by the TEM observation during correlative microscopy.

Correlative microscopy allows the combination of different microscopic methods to bridge the macrostructural analysis like light microscopy (morphological orientation and information) with the nanostructural analysis like TEM for clear characterisations of special spots with ultra high resolution within ROIs. Furthermore, the correlative workflow allows examination of the same sample for all methods of each step of the workflow.

Correlative microscopy was applied in this study to confirm the uptake of AgNPs by *H. azteca* and to further elucidate the potential tissue penetration and accumulation of the ingested particles. TEM observations, which are carried out as part of the correlative microscopy workflow, allow detection of particulate Ag without false detection of Ag that is complexed or associated with organic matter (Kampe et al., 2018). Thus the risk of detecting artifacts, like the measurement of pseudoparticles, is not possible. Even though correlative microscopy provides results which are not quantitative, the methods applied allow a precise localization and characterization (indication of

Table 3
Particle concentrations (particles/L) in the media samples from day 4 and 7, and animals tissue from day 7. Diameter of particles in the samples were calculated median diameters in nm.

Treatment	Matrix	Concentration [particles/L]		Diameter [nm]	
		Day 0	Day 7	Day 0	Day 7
S_0	Media	–	–	–	–
	Animals	–	$2.2 \times 10^8 \pm 1.5 \times 10^7$	–	17.2 ± 0.2
S_L	Media	$3.7 \times 10^8 \pm 3.0 \times 10^7$	$1.5 \times 10^{11} \pm 2.2 \times 10^9$	11.5 ± 0.2	15.0 ± 0.0
	Animals	–	$2.5 \times 10^{12} \pm 3.4 \times 10^{11}$	–	18.5 ± 0.4
$AgNO_3$	Media	$5.0 \times 10^9 \pm 2.0 \times 10^9$	$6.0 \times 10^9 \pm 4.6 \times 10^9$	11.2 ± 0.5	13.5 ± 0.8
	Animals	–	$8.2 \times 10^9 \pm 4.6 \times 10^9$	–	17.6 ± 1.2

transformation) of the NPs. In this way it was shown that there were only very low amounts of AgNPs in the gut of the amphipods (S_L treatment) and no AgNPs within the animals tissue. Also, no AgNPs were found in the animals with no direct contact to AgNP enriched sludge. From this it can be concluded, that the AgNPs were only taken up from the sludge, but not incorporated into the organisms tissue or cells. Furthermore, the correlative microscopy revealed that the quantification of the Ag body burden by ICP-OES and spICP-MS was not influenced by NPs attached to the carapace. Thus the measured Ag body burden only represents the AgNPs in the gut content and potentially other Ag species like Ag^+ in non particulate form which were taken up via bioconcentration processes.

By using the method of spICP-MS high concentrations of measured particles (< 20 nm) were found in animals collected from control and all treatments at the end of the second study. However, no Ag particles could be identified by correlative microscopy in control animals even though a low level of Ag was detected in the tissue. This was potentially caused by the ingestion of the control sludge containing a low amount of silver as background contamination. Animals collected from the S_L strainer group, without direct contact to the STP sludge containing high Ag concentrations, showed accumulation of silver. However, no Ag particles could be observed in the animals using correlative microscopy providing clear evidence that Ag was supposed to be accumulated following uptake of Ag^+ ions released from the sludge.

As described for several invertebrates and aquatic species, the bioaccumulation of Ag, especially after the exposure of Ag ions, occurs rapidly and often leads to high body burdens, due to effective and active uptake mechanisms and binding of Ag to proteins as a detoxification strategy (Croteau et al., 2011; Hogstrand et al., 1996; Kuehr et al., 2020; Waalewijn-Kool et al., 2014). Also in this study, Ag^+ accumulated by bioconcentration processes or incorporated after release from the gut content seems to be associated to proteins like metallothioneins (Ahearn, 2010). This could explain, why around 57% of the total amount of the Ag body burden found in the animals collected from the $AgNO_3$ treatment was detected in the protein solution prepared from the same sample material. In comparison, only 17% of the total amount of Ag found in animals from the S_L treatment, with direct contact to the contaminated sludge, was detected in the animals protein fraction which may be explained by the lower concentration of Ag^+ due to the limited and delayed release of Ag^+ from the sulfidized AgNP surface.

Nevertheless, the measured accumulation of Ag in the groups separated in strainers was very limited. This can be explained by the observation that Ag^+ released from the sludge was apparently not freely dissolved as confirmed by the $AgNO_3$ treatment. The results of Ag measurements following ultrafiltration of the S_L media from the first and second exposure tests have both shown that around 99% of the total silver measured in the medium was present in a particulate or colloidal form that could not pass through 3 kD filter membrane. This could be explained by precipitates, suspended AgNPs, or Ag^+ bound to humic acids, proteins or other organic colloids (Degenkolb et al., 2018; Kaegi et al., 2011; Kampe et al., 2018). The assumption that Ag^+ is associated with organic or inorganic colloids is in agreement with the observation that around 99% of the measured total Ag in the medium of the $AgNO_3$ treatment were also present in a particulate form or associated with colloids bigger than 3 kD as shown by ultrafiltration.

The test design used for this study allowed investigation of the major pathways involved in the accumulation of Ag from AgNPs in STP sludge. The calculation of accumulation factors as the ratio of total Ag concentrations in the aqueous media helped to evaluate the impact of dietary uptake and bioconcentration processes leading to the Ag accumulation in *H. azteca* observed in this study.

No significant difference between the AF_M values of the top and bottom group of the $AgNO_3$ treatment was observed (363 vs. 396). Both groups were kept in contact with control sludge and exposed to the same test medium. In contrast, AF_M values calculated for the S_L treatment (second study) reveal that there was a significant difference regarding the accumulation of Ag in the top and bottom group (376 vs. 39,404). Groups of both treatments (S_L and $AgNO_3$) were exposed to the same medium concentration, but fed on different types of sludge in the bottom group underlining the major contribution of dietary uptake to the measured Ag body burden and the apparent accumulation of Ag in this exposure scenario.

AF_M values observed in the S_L treatment from the second exposure study confirm the significant difference in the calculated AF_M values regarding the accumulation of Ag in the top and bottom group (504 and 21,730). However, AF_M values calculated for the animals in the strainer (top) were higher compared to the first study. During the first and second study sludge with the same concentration was applied in the S_L treatment but leading to different media concentrations. This may be explained by the different amount of sludge that was provided to the vials to guarantee feeding ad libitum of the test animals. Bigger animals were exposed during the second study. Consequently, the application of the higher amount of sludge during the second study led to higher total Ag concentrations in the test media compared to the first test as reflected in the AF_M values.

Ag^+ is well known to induce lethal and sublethal toxicological effects, especially in aquatic species (Leblanc et al., 1984; Sakamoto et al., 2015; Wang et al., 2012; Zhao and Wang, 2011). However, no mortality or significant effects were observed in both exposure studies. The presumable complexion of Ag^+ from the $AgNO_3$ treatment and potentially released Ag^+ from AgNPs of the enriched sludges may explain the lack of significant effects or mortality in comparison to the S_0 control group in both studies, even if *H. azteca* is considered to be the most sensitive benthic species for Ag^+ exposure (Blaser et al., 2008). The lack of observed effects is in accordance with the results of Kühr et al. 2018, where the waste water borne AgNPs did not cause any negative effects in contrast to water borne pristine AgNPs. Comparable observations were made by Hartmann et al. (2019) when pristine AgNPs from NM 300 K caused a significant reduction of the reproduction in *Daphnia magna*, while wastewater borne NM 300 K AgNPs, which were proved to be transformed to Ag_2S, did not cause any significant differences in the number of offspring (Hartmann et al., 2019).

5. Conclusions

AgNPs such as NM 300K can be ingested by the benthic amphipod *Hyalella azteca* by dietary uptake from STP sludge as shown in this study. However, even though the NPs were shown to be ingested, we did not find any evidence for an incorporation of the NPs or transfer from the gut into the animals tissue or cells. However, the bioaccumulation of Ag^+ released from the sulfidized AgNPs, was confirmed. The accumulation of Ag from AgNPs may lead to a higher Ag body burden in the animals and the amphipods may thus accelerate the transfer of heavy metals from NPs accumulated in the sediment into the aquatic food chain (Vogt et al., 2019).

It was shown that investigations on the bioavailability and bioaccumulation of NPs in aquatic organisms should be complemented by the methods of correlative microscopy. The reason for this is that the established method of spICP-MS often detects artifacts, such as presumable and/or pseudo particles, but cannot confirm (or conclude) that they are in fact artifacts. Further investigations utilizing imaging methods with higher resolution, such like synchrotron radiation x-ray imaging, are required to gain more information on the distribution of the metal within the organism to allow a more precise conclusionon the bioavailability and bioaccumulation of AgNPs.

Funding

This research did not receive any specific grant from funding agencies in the public, commercial, or not-for-profit sectors.

Abbreviations

AF_M	Accumulation factor based on the Ag concentration in the medium
Ag^+	Silver (I) ion
AgNPs	Silver nanoparticles
ANOVA	Analysis of variance
BSE	Backscattered electron
EDX	Energy dispersive x-ray spectroscopy
SP-ICP-MS	Single particle inductively coupled plasma mass spectrometry
ICP-MS	Inductively coupled plasma mass spectrometry
ICP-OES	Inductively coupled plasma optical emission spectrometry
NP	Nanoparticle
OECD	Organization for Economic Co-Operation and Development
PMMA	Polymethylmethacrylate
ROI	Region of interest
SEM	Scanning electron microscopy
STP	Sewage treatment plant
TEM	Transmission electron microscopy
TWA	Time weighted average concentration
UHQ water	Ultra high quality water

CRediT authorship contribution statement

Sebastian Kuehr: Methodology, Investigation, Writing - review & editing.**Jessica Klehm:**Methodology, Investigation, Visualization, Writing - review & editing.**Claudia Stehr:**Methodology.**Matthias Menzel:**Methodology.**Christian Schlechtriem:**Writing - review & editing, Supervision.

Declaration of competing interest

The authors declare that they have no known competing financial interests or personal relationships that could have appeared to influence the work reported in this paper.

Acknowledgements

This work was financially supported by the Fraunhofer Institute for Molecular Biology and Applied Ecology IME and the Fraunhofer Institute for Microstructure of Materials and Systems IMWS. We thank Nicola Schröder for supporting the sp-ICP-MS measurements and Virginia Schraps, Lara Hermsen and Richard Zeumer for their help during the measurements of total Ag concentrations. We thank four unknown reviewers for their valuable comments on the manuscript.

Appendix A. Supplementary data

Supplementary data to this article can be found online at https://doi.org/10.1016/j.impact.2020.100239.

References

Adam, V., Nowack, B., 2017. European country-specific probabilistic assessment of nanomaterial flows towards landfilling, incineration and recycling. Environ.Sci:Nano 4, 1961. https://doi.org/10.1039/c7en00487g.

Ahearn, G.A., 2010. In: Zalups, R.K., Koropatnick, J. (Eds.), Cellular and Molecular Biology of Metals. Taylor and Francis, London. CRC Press, pp. 295–326.

Alves, L.C., Borgmann, U., Dixon, D.G., 2009a. Kinetics of uranium uptake in soft water and the effect of body size, bioaccumulation and toxicity to *Hyalella azteca*. Environ. Pollut. 157, 2239–2247.

Alves, L.C., Borgmann, U., Dixon, D.G., 2009b. Kinetics of uranium uptake in soft water and the effect of body size, bioaccumulation and toxicity to *Hyalella azteca*. Environ. Pollut. 157, 2239–2247.

Bianchini, A., Wood, C.M., 2008. Does sulfide or water hardness protect against chronic silver toxicity in *Daphnia magna*? A critical assessment of the acute-to-chronic toxicity ratio for silver. Ecotoxicol. Environ. Saf. 71, 32–40.

Bianchini, A., Bowles, K.C., Brauner, C.J., Gorsuch, J.W., Kramer, J.R., Wood, C.M., 2002. Evaluation of the effect of reactive sulfide on the acute toxicity of silver (I) to *Daphnia magna*. Part 2: toxicity results. Environ. Toxicol. Chem. 21, 1294–1300.

Blaser, S.A., Scheringer, M., MacLeod, M., Hungerbühler, K., 2008. Estimation of cumulative aquatic exposure and risk due to silver: contribution of nano-functionalized plastics and textiles. Sci. Total Environ. 390, 396–409.

Bradley, R.S., Withers, P.J., 2016. Correlative multiscale tomography of biological materials. MRS Bull. 41, 549–554.

Bundschuh, M., Filser, J., Lüderwald, S., McKee, M.S., Metreveli, G., Schaumann, G.E., Schulz, R., Wagner, S., 2018. Nanoparticles in the environment: where do we come from, where do we go to? Environ. Sci. Eur. 30, 6.

Burkhardt, M., Zuleeg, S., Ka, R., Sinnet, B., Eugster, J., Boller, M., Siegrist, H., 2010. Verhalten von Nanosilber in Kläranlagen und dessen Einfluss auf die Nitrifikationsleistung in Belebtschlamm. Umweltwissenschaften und Schadstoff-forsch 22, 529–540.

Caplan, J., Niethammer, M., Taylor, R.M., Czymmek, K.J., 2011. the power of correlative microscopy: multi-modal, multi-scale, multi-deimensional. Curr. Opin. Struct. Biol. 21, 686–693.

Choi, O., Hu, Z., 2008. Size dependent and reactive oxygen species related nanosilver toxicity to nitrifying bacteria. Environ. Sci. Technol. 42, 4583–4588.

Croteau, M.N., Misra, S.K., Luoma, S.N., Valsami-Jones, E., 2011. Silver bioaccumulation dynamics in a freshwater invertebrate after aqueous and dietary exposures to nanosized and ionic Ag. Environ. Sci. Technol. https://doi.org/10.1021/es200880c.

Degenkolb, L., Metreveli, G., Philippe, A., Brandt, A., Leopold, K., Zehlike, L., Vogel, H.-J., Schaumann, G.E., Baumann, T., Kaupenjohann, M., Lang, F., Kumahor, S., Klitzke, S., 2018. Retention and remobilization mechanisms of environmentally aged silver nanoparticles in an artificial riverbank filtration system. Sci. Total Environ. 645, 192–204.

Donath, K., 1995. Preparation of Histologic Sections. vol. 16. Nord. EXAKT-Kulzer Publ, pp. 16.

Future Markets Inc, 2017. The Global Market for Metal and Metal Oxide Nanoparticles 2010–2027.

Gottschalk, F., Nowack, B., 2011. The release of engineered nanomaterials to the environment. J. Environ. Monit. 13, 1145.

Guérin, C.J., Liv, N., Klumperman, J., 2019. Correlative Imaging. Wiley, pp. 1–21.

Hartmann, S., Louch, R., Zeumer, R., Steinhoff, B., Mozhayeva, D., Engelhard, C., Schönherr, H., Schlechtriem, C., Witte, K., 2019. Comparative multi-generation study on long-term effects of pristine and wastewater-borne silver and titanium dioxide nanoparticles on key lifecycle parameters in *Daphnia magna*. NanoImpact 14, 100163. https://doi.org/10.1016/j.impact.2019.100163.

Hogstrand, C., Galvez, F., Wood, C.M., Morgan, T.H., 1996. Toxicity, silver accumulation and metallothionein induction in freshwater rainbow trout during exposure to different silver salts. Environ. Toxicol. Chem. 15, 1102–1108.

Impellitteri, C.A., Harmon, S., Silva, R.G., Miller, B.W., Scheckel, K.G., Luxton, T.P., Schupp, D., Panguluri, S., 2013. Transformation of silver nanoparticles in fresh, aged, and incinerated biosolids. Water Res. 47, 3878–3886.

Kaegi, R., Voegelin, A., Sinnet, B., Zuleeg, S., Hagendorfer, H., Burkhardt, M., Siegrist, H., 2011. Behavior of metallic silver nanoparticles in a pilot wastewater treatment plant. Environ. Sci. Technol. 45, 3902–3908.

Kaegi, R., Voegelin, A., Ort, C., Sinnet, B., Thalmann, B., Krismer, J., Hagendorfer, H., Elumelu, M., Mueller, E., 2013. Fate and transformation of silver nanoparticles in urban wastewater systems. Water Res. 47, 3866–3877.

Kampe, S., Kaegi, R., Schlich, K., Wasmuth, C., Hollert, H., Schlechtriem, C., 2018. Silver nanoparticles in sewage sludge: bioavailability of sulfidized silver to the terrestrial isopod *Porcellio scaber*. Environ. Toxicol. Chem. https://doi.org/10.1002/etc.4102.

Kim, S., Choi, J.E., Choi, J., Chung, K.-H., Park, K., Yi, J., Ryu, D.-Y., 2009. Oxidative stress-dependent toxicity of silver nanoparticles in human hepatoma cells. Toxicol. in Vitro 23, 1076–1084.

Klein, C.L., Stahlmecke, B., Romazanov, J., Kuhlbusch, T.A.J., Van Doren, E., De Temmerman, P.-J., Mast, J., Wick, P., Krug, H., Locoro, G., Hund-Rinke, K., Kördel, W., Friedrichs, S., Maier, G., Werner, J., Linsinger, T., Gawlik, B.M., Comero, S., Institute for Health and Consumer Protection, European Commission, Joint Research Centre, Institute for Environment and Sustainability, Institute for Reference Materials and Measurements, 2011. NM-Series of Representative Manufactured Nanomaterials: NM-300 Silver Characterisation, Stability, Homogeneity. Publications Office.

Kraas, M., Schlich, K., Knopf, B., Wege, F., Kägi, R., Terytze, K., Hund-Rinke, K., 2017. Long-term effects of sulfidized silver nanoparticles in sewage sludge on soil microflora. Environ. Toxicol. Chem. 36, 3305–3313.

Kuehr, S., Meisterjahn, B., Schröder, N., Knopf, B., Völker, D., Schwirn, K., Schlechtriem, C., 2020. Testing the bioaccumulation of manufactured nanomaterials in the freshwater bivalve *Corbicula fluminea* using a new test method. Environ. Sci. Nano 7, 535–553. https://doi.org/10.1039/C9EN01112A.

Kühr, S., Schneider, S., Meisterjahn, B., Schlich, K., Hund-Rinke, K., Schlechtriem, C., 2018. Silver nanoparticles in sewage treatment plant effluents: chronic effects and accumulation of silver in the freshwater amphipod *Hyalella azteca*. Environ. Sci. Eur. 30, 7.

Leblanc, G.A., Mastone, J.D., Paradice, A.P., Wilson, B.F., Jr, H.B.L., Robillard, K.A., 1984. The influence of speciation on the toxicity of silver to fathead minnow (*Pimephales promelas*). Environ. Toxicol. Chem. 3, 37–46.

Lee, S., Bi, X., Reed, R.B., Ranville, J.F., Herckes, P., Westerhoff, P., 2014. Nanoparticle size detection limits by single particle ICP-MS for 40 elements. Environ. Sci. Technol. 48, 10291–10300.

Levard, C., Hotze, E.M., Lowry, G.V., Brown, G.E., 2012. Environmental transformations of silver nanoparticles: impact on stability and toxicity. Environ. Sci. Technol. 46, 6900–6914.

European Commission, Nanotechnology: research and innovation the invisible giant tackling Europe's future challenges. 2013.

Liu, J., Hurt, R.H., 2010. Ion release kinetics and particle persistence in aqueous nanosilver colloids. Environ. Sci. Technol. https://doi.org/10.1021/es9035557.

Loeschner, K., Navratilova, J., Købler, C., Mølhave, K., Wagner, S., von der Kammer, F., Larsen, E.H., 2013. Detection and characterization of silver nanoparticles in chicken meat by asymmetric flow field flow fractionation with detection by conventional or single particle ICP-MS. Anal. Bioanal. Chem. 405, 8185–8195.

Lombi, E., Donner, E., Taheri, S., Tavakkoli, E., Jämting, Å.K., McClure, S., Naidu, R., Miller, B.W., Scheckel, K.G., Vasilev, K., 2013. Transformation of four silver/silver chloride nanoparticles during anaerobic treatment of wastewater and post-processing of sewage sludge. Environ. Pollut. 176, 193–197.

Loussert Fonta, C., Humbel, B.M., 2015. Correlative microscopy. Arch. Biochem. Biophys. 581, 98–110.

Mulisch, M., Sauer, U., 2015. Romeis - Mikroskopische Technik. Springer Berlin Heidelberg, pp. 63–76.

Nuutinen, S., Landrum, P.F., Schuler, L.J., Kukkonen, J.V.K., Lydy, M.J., 2003. Toxicokinetics of organic contaminants in *Hyalella azteca*. Arch. Environ. Contam. Toxicol. 44, 467–475.

Organisation for Economic Co-operation and Develpement (OECD), 2001. Test No. 303: Simulation Test - Aerobic Sewage Treatment - A: Activated Sludge Units; B: Biofilms. OECD.

Othman, M.S., Pascoe, D., 2001. Growth, development and reproduction of *Hyalella azteca* (Saussure, 1858) in laboratory culture. Crustaceana 74, 171–181.

PEN, 2013. Project on emerging nanotechnologies. http://www.nanotechproject.org/, Accessed date: 14 June 2018.

Raths, J., Kuehr, S., Schlechtriem, C., 2020. Bioconcentration, metabolism, and spatial distribution of ^{14}C-labeled laurate in the freshwater amphipod *Hyalella azteca*. Environ. Toxicol. Chem. 39 (2), 310–322 (etc.4623).

Reinsch, B.C., Levard, C., Li, Z., Ma, R., Wise, A., Gregory, K.B., Brown, G.E., Lowry, G.V., 2012. Sulfidation of silver nanoparticles decreases *Escherichia coli* growth inhibition. Environ. Sci. Technol. 46, 6992–7000.

Sakamoto, M., Ha, J.Y., Yoneshima, S., Kataoka, C., Tatsuta, H., Kashiwada, S., 2015. Free silver ion as the main cause of acute and chronic toxicity of silver nanoparticles to cladocerans. Arch. Environ. Contam. Toxicol. 68, 500–509.

Schlechtriem, C., Kampe, S., Bruckert, H.-J., Bischof, I., Ebersbach, I., Kosfeld, V., Kotthoff, M., Schäfers, C., L'Haridon, J., 2019. Bioconcentration studies with the freshwater amphipod *Hyalella azteca*: are the results predictive of bioconcentration in fish? Environ. Sci. Pollut. Res. 26, 1628–1641.

Schlich, K., Klawonn, T., Terytze, K., Hund-Rinke, K., 2013. Hazard assessment of a silver nanoparticle in soil applied via sewage sludge. Environ. Sci. Eur. 25, 17.

Schmidt, B., Loeschner, K., Hadrup, N., Mortensen, A., Sloth, J.J., Bender Koch, C., Larsen, E.H., 2011. Quantitative characterization of gold nanoparticles by field-flow fractionation coupled online with light scattering detection and inductively coupled plasma mass spectrometry. Anal. Chem. 83, 2461–2468.

Starnes, D.L., Lichtenberg, S.S., Unrine, J.M., Starnes, C.P., Oostveen, E.K., Lowry, G.V., Bertsch, P.M., Tsyusko, O.V., 2016. Distinct transcriptomic responses of *Caenorhabditis elegans* to pristine and sulfidized silver nanoparticles. Environ. Pollut. 213, 314–321.

Verkade, P., Collinson, L., 2019. Correlative Imaging: Focusing on the Future. John Wiley & Sons.

Vogt, R., Mozhayeva, D., Steinhoff, B., Schardt, A., Spelz, B.T.F., Philippe, A., Kurtz, S., Schaumann, G.E., Engelhard, C., Schönherr, H., Lamatsch, D.K., Wanzenböck, J., 2019. Spatiotemporal distribution of silver and silver-containing nanoparticles in a prealpine lake in relation to the discharge from a wastewater treatment plant. Sci. Total Environ. 696, 134034. https://doi.org/10.1016/j.scitotenv.2019.134034.

Waalewijn-Kool, P.L., Klein, K., Forniés, R.M., van Gestel, C.A.M., 2014. Bioaccumulation and toxicity of silver nanoparticles and silver nitrate to the soil arthropod *Folsomia candida*. Ecotoxicology 23, 1629–1637.

Wang, Z., Chen, J., Li, X., Shao, J., Peijnenburg, W.J.G.M., 2012. Aquatic toxicity of nanosilver colloids to different trophic organisms: contributions of particles and free silver ion. Environ. Toxicol. Chem. 31, 2408–2413.

Wasmuth, C., Rüdel, H., Düring, R.-A., Klawonn, T., 2016. Assessing the suitability of the OECD 29 guidance document to investigate the transformation and dissolution of silver nanoparticles in aqueous media. Chemosphere 144, 2018–2023.

West, R., 1996. CRS Handbook of Chemistry and Physics: A Ready-reference Book of Chemical and Physical Data, 67th editon. CRC Press, Boca Raton.

Zeumer, R., Hermsen, L., Kaegi, R., Kuehr, S., Knopf, B., Schlechtriem, C., 2020. Bioavailability of silver from wastewater and planktonic food borne silver nanoparticles in the rainbow trout *Oncorhynchus mykiss*. Sci. Total Environ. 706, 135695 doi:Bioavailability of silver from wastewater and planktonic food borne silver nanoparticles in the rainbow trout Oncorhynchus mykiss.

Zhao, C.-M., Wang, W.-X., 2011. Comparison of acute and chronic toxicity of silver nanoparticles and silver nitrate to *Daphnia magna*. Environ. Toxicol. Chem. 30, 885–892.